2021 43rd Annual International Conference of the
IEEE Engineering in Medicine & Biology Society (EMBC)
Oct 31 - Nov 4, 2021. Virtual Conference

A disposable force regulation mechanism for throat swab robot

Zhuoqi Cheng and Thiusius Rajeeth Savarimuthu

***Abstract*— Robots can protect healthcare workers from being infected by the COVID-19 and play a role in throat swab sampling operation. A critical requirement in this process is to maintain a constant force on the tissue for ensuring a safe and good sampling. In this study, we present the design of a disposable mechanism with two non-linear springs to achieve a 0.6 N constant force within a 20 mm displacement. The non-linear spring is designed through optimization based on Finite Element Simulation and Genetic Algorithm. Prototype of the mechanism is made and tested. The experimental results show that the mechanism can provide 0.67±0.04 N and 0.57±0.02 N during its compression and return process. The proposed design can be extended to different scales and used in a variety of scenario where safe interacting with human is required.**

I. Introduction

Since the end of 2019, the world has been hit by the novel corona virus (COVID-19), making many people being absent from normal life and causing a lot of deaths everyday. Almost all the countries have approved essential diagnostic testing to find out if a people is currently infected with the virus. One of the most generic testings is done by inserting a long cotton stick into the back of throat for collecting saliva samples. A positive test results is considered if the genetic material of the virus is detected. So far, all the throat swab sampling procedures are done by healthcare workers who are at high risk of infection and potentially contributing to further spread. Thus, there is an on-going need to reduce the workload of the healthcare worker and protect them from virus transmission.

Back in May 2020, the medical robotics lab in the University of Southern Denmark claims the development of the world's first fully automatic throat swab robot, and it leads to a spin-off company called Lifeline Robotics [1]. As shown in Fig. 1, the SDU throat swab robot provides autonomous throat swab operation including swab region detection based on stereo-vision, vision guided cotton stick insertion, force based control swabbing and transferring sample to a burette. In addition to the SDU throat swab robot, other research institutes have proposed and developed related robotic platforms for pharynx or nasopharyngeal swab sampling including [1], [2], [3].

In order to promote the above robots to practical use, it is essential to satisfy the requirements related to safe human-robot contact and instrument sterilization. The exerting force on the throat from the cotton stick should be constrained: it should be big enough to ensure a stable swab, but also small enough to avoid causing uncomfortable feeling or injury. Therefore, close-loop position-force control is required during the process. However, since the mouth cavity is narrow, the vision is often occluded. The control of contact heavily relies on the force sensing between the robot's end-effector and the cotton stick holder. In practice, the operating robot should be draped to fulfil the sterilization requirements. This can potentially increase the noise level for the force sensing, and thus leading to unsafe or unreliable contact. In addition, throat is a sensitive region and muscle contraction often occurs during the swab procedure. This kind of artifact is generally difficult to compensate in a control system due to high acceleration.

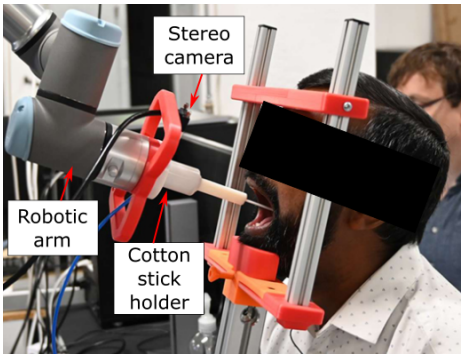

Fig. 1. Prototype of the SDU throat swab robot.

This study presents the design of a disposable mechanism to provide constant force, and it can be easily manufactured, assembled, sterilized and use. Different constant force mechanisms design methods have been proposed previously based on topological optimization specifically on the structure, beam shape, and beam thickness [4], [5], [6], [7]. In this study, the force regularization is achieved by a set of non-linear springs which are designed through an optimization process consisting of Genetic Algorithm (GA) and Finite Element Simulation (FES) [8]. Compared to the previous methods [4], [8], the method presented in this study seeks a spring shape to output a constant force instead of matching a series of specific force values. This can improve the convergent efficiency. Then through adjusting the cross-section shape, the force magnitude can be amplified to the required value. Subsequently, the whole mechanism is developed upon the non-linear spring, and it can be fabricated in a fast and low cost way.

After the introduction in Section I, Section II describes the design method of the non-linear spring. In Section III, a prototype of the mechanism is made, and it is evaluated

Z. Cheng and T.R. Savarimuthu are with the Mærsk Mc Kinney Møller Instituttet, University of Southern Denmark.
Corresponding author: Zhuoqi Cheng (email: zch@mmmi.sdu.dk)
[1]https://www.lifelinerobotics.com/

through experiments which is provided in Section IV. Section V discusses the results and concludes the whole paper.

II. Method

A. Design specifications

As mentioned above, the mechanism aims to regulate the contacting force on the throat during the swab procedure. Specifically, the mechanism should maintain a constant force when the muscle contraction of the pharynx happens. Based on our preliminary trials, the expected output force is specified to be 0.6 N, and the muscle contraction is estimated to be within a displacement of 20 mm. In addition, the mechanism should be manufactured fast and in a low cost. Little efforts for assembly should be accounted so that the sterilization process can be greatly simplified.

The key components of the proposed mechanisms are the nonlinear springs which offer a constant output force within a required distance. The schematic of the nonlinear spring design is illustrated in Fig. 2. The design procedure of the nonlinear spring includes two steps. Step 1 seeks some proper spring shapes with a constant force output. In this step, the magnitude of the output force is not required to be the same as the required value in order to speed up the result convergence. In step 2, the cross-section of the spring is adjusted to make the output force equal to the required magnitude. During the cross-section design, the max stress is checked and ensured not exceeding the material's limit.

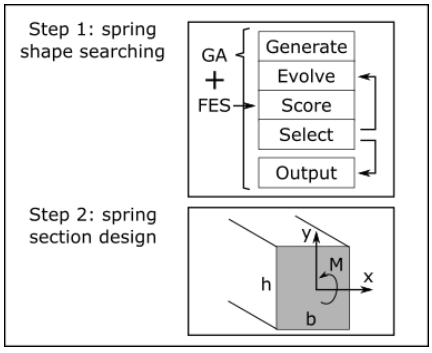

Fig. 2. Approach to generate the design of the compliant beam: In Step 1, an optimisation procedure including GA and FES runs to obtain a good spring shape which can output a constant force; In Step 2, the cross-section of the spring is optimized to closely match to the required value.

B. Step 1: stiffness optimization

The design method of this study is an improved version based on the previous study [9]. Naturally, designing the shape of a non-linear spring with a specific stiffness function is not intuitive. Therefore, we propose to exploit GA and FES for the design optimization. GA offers a straightforward way for generating and comparing different viable solutions (spring shapes), and loops until the cost of the objective function reaches an acceptable threshold. Thanks to its relatively unconstrained nature of the searching capability, GA offers more generic benefits of avoiding local minimal. In addition, FES allows to estimate the stiffness function (reacting force against displacement) of a specific shape of the nonlinear spring fast and accurately. More technical details are given as follows.

1) Objective function formulation: The nonlinear spring is expected to output a constant force within a pre-defined stroke in this application. As shown in Fig. 3, we select n sampling points in a series of displacements, which are used for evaluating the generated nonlinear spring' performance. The sampling starts from displacement of 15 mm, before which is considered for the force increment. Then, we evaluate the constancy of the output force from 15 mm to 40 mm. Here, we set 5 mm more for safety margin. The cost function is defined as the relative standard deviation of all the sampling points:

$$\text{Minimise } \Phi = \frac{STD(\{F_1, ..., F_n\})}{Avg.(\{F_1, ..., F_n\})} \tag{1}$$

where $\{F_1, ..., F_n\}$ represent the actual forces of a serials of evaluation points.

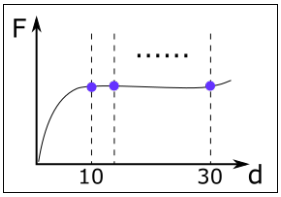

Fig. 3. The objective of the optimization is to minimize the relative standard deviation of the stiffness function in the region of interest.

2) Finite Element Analysis: To estimate the output force against the displacement for each candidate spring, FES based on ANSYS APDL command is used. In the simulation, the material elements satisfy the following equation:

$$[K]\{u\} = \{F\} \tag{2}$$

where [K] is the stiffness matrix, $\{u\}$ is the displacement of elements and $\{F\}$ is the external force matrix.

Large deformation is activated, and nonlinear FEA is involved automatically for this feature. The overall load is divided into several increments, and applied over several steps. Also, the stiffness matrix is updated in each iteration according to the displacement $\{u\}$. The Newton-Raphson Method is used to solve the stiffness matrix $[K_i]$ and the displacement of next iteration $\{u_{i+1}\}$ (i indicates the iteration number) iteratively as follows:

$$[K_i]\{\Delta u_i\} = \{F\} - \{\Delta F_i\} \tag{3}$$

$$\{u_{i+1}\} = \{u_i\} + \{\Delta u_i\} \tag{4}$$

Here, we set the cross-section of the spring as 0.4×0.4 mm which is the minimum resolution for the 3D printer nozzle.

3) Genetic Algorithm optimisation: Genetic algorithm is involved for seeking the optimal shapes of with the minimum Φ value. As depicted in Fig. 2, the optimisation procedure includes 4 main steps: generate, evolve, score, and select.

The algorithm starts with generating a bunch of spring shapes randomly. Each spring shape is defined as a cubic spline parameterized by five key points inside a predefined boundary. Through some trials, we decided to use five key points for defining a spring shape because such a spline is neither too winding nor too straight so as to have enough stiffness diversity. These five key points (x_i, y_i) are represented by a chromosome $C_i = [x_{i1}, y_{i1}, x_{i2}, y_{i2}, x_{i3}, y_{i3}, x_{i4}, y_{i4}, x_{i5}, y_{i5}]$. Specifically, point $[x_{i1}, y_{i1}]$ and point $[x_{i5}, y_{i5}]$ are the start and end points respectively which are fixed and decided by the user at the beginning. Subsequently, a self-intersection test of the generated curve is conducted. Considering the feasibility of fabrication, only those past the test are selected to the mating pool.

There are two main methods involved in the evolution process, namely crossover and mutation. The crossover procedure generates new chromosomes to the mating pool based on two existing chromosomes. One of the three middle key points is randomly selected of these two chromosomes, and then they exchange their left part with the right part remaining. In this study, the occurrence probability of crossover is set to be $p_c = 0.3$. In addition, a mutation process is implemented to tune the key points of the selected chromosomes within a small region. During this procedure, the positions of the three middle key points are updated by multiplying random numbers based on Gaussian distribution ($\mu = 1, \sigma = 0.01$).

$$C_i^t = C_i^{t-1} \cdot N(1, 0.01^2) \tag{5}$$

The score of each chromosome is given according to the objective function. If there are chromosomes in the pool with scores lower than the preset threshold, the loop is finished and these chromosomes are output as the optimal spring shape. Otherwise, the Roulette Wheel Selection Method is used for removing a portion of chromosomes from the pool. Chromosomes with smaller Φ value are assigned a larger share of the roulette wheel representing a higher survival rate in the pool. To maintain the quantity of chromosomes in the mating pool, new chromosomes are generated and added to the pool. The above process is believed to avoid local optimum convergence effectively.

C. Step 2: section design

Subsequently, the cross-section of the spring is designed to amplify the output force. In this study, rectangular section is used to simplify the design. The stiffness of the spring can be scaled through the increment of the width b or the thickness h. On the one hand, the stiffness is more sensitive to the change of h. However, increasing h can also lead to a significant increase of the maximum stress during the deformation. On the other hand, the scale of the stiffness is gentle and proportional to b. Therefore, the tuning of these two parameters aims to reach a balance between the maximum stress and compact structure. A suggested procedure is to first increase the h until the maximum stress is close to the safety margin of the material. Then b is adjusted to ensure the spring outputs the required force magnitude. The above design procedure is also done through FES using ANSYS, and the material of the spring is the default setting of PLA in the software.

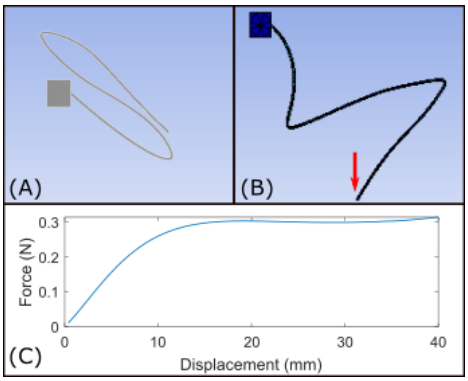

Fig. 4. (A) The optimized spring shape; (B) The deformation of the spring after 25 mm displacement; (C) The stiffness function of the generated spring.

III. Prototype and Assembly

Two springs are used in the mechanism for balancing the lateral forces. Thus, each spring is required to output a constant force of 0.3 N. After the above design procedure, one of the beam shapes is selected for this application as shown in Fig. 4(A). The thickness and the width of the spring are 0.8 mm and 2.7 mm respectively. The simulation of the spring deformation with the end moving 40 mm downwards is shown in Fig. 4(B). According to the FES results, the maximum stress is found to be 69 MPa which is smaller than 70% of the tensile yields strength of PLA (106 MPa). Also, the resultant force-displacement property of the spring is presented in Fig. 4(C). After a pre-load of 15 mm, a subsequent 25 mm of constant force (about 0.3 N) can be achieved. The relative standard deviation of the output force within the last 25 mm displacement is found to be 0.3±0.004 N.

Fig. 5(A) shows the whole mechanisms include four components: two nonlinear springs, a base frame and a slider. The base frame is used to fix one end of the springs and has two columns to guide the movement of the slider. On the top of each column, a small pawl is made to stop the slider, which also provides the 15 mm pre-load. All the components are designed for fabrication using 3D printing or molding. The prototype is made as seen in Fig. 5(B). The assembly procedure include inserting two springs to the slots on the base frame, inserting the slider to the column guide and connecting the hole of the spring's end to the pin of the slider. The assembling process can be easily accomplished within a minute, and the total cost is estimated to be less than 10 Euro.

IV. Experiment and Results

An experiment was designed to evaluate the performance of the mechanism. As shown in Fig. 6, a UR3 robot was used for pushing the constant force mechanism downwards

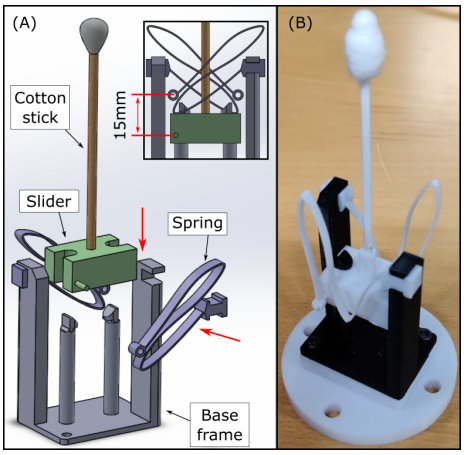

Fig. 5. The assembly diagram (A) and the prototype (B) of the mechanism.

and controlling the displacement. A cotton stick was inserted to the hole of the slider, and its tip was adjusted to contact a force sensor (FSAGPNXX1.5LC, Honeywell Inc., US) vertically. During the experiment, the robot first pushed the cotton stick 20 mm downwards in 2 mm/s and then raised up 20 mm in the same speed. During this procedure, the pushing force was recorded via a Data Acquisition (Arduino Uno, Arduino S.r.l., Italy) in real time. This experiment was repeated 5 times.

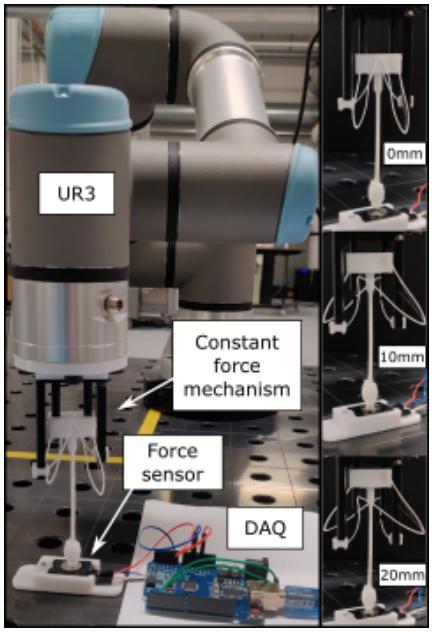

Fig. 6. Experiment setup to evaluate the performance of the designed mechanism.

The mean value and standard deviation of the recorded force is shown in Fig. 7. The blue curve and the red curve represents the force-displacement values when the mechanism is compressed and returns respectively. The compression force and return force over the whole stroke is calculated to be 0.67±0.04 N and 0.57±0.02 N respectively.

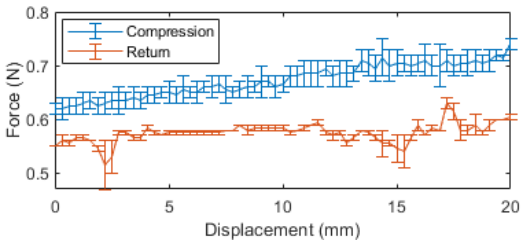

Fig. 7. The output force during the compression and return process of the mechanism.

V. Discussion and Conclusion

In this study, we present the design of a force regulation mechanism which can be used to provide a 0.6 N constant force during the throat swab sampling. The whole mechanism includes two nonlinear springs, a base frame and a slider. Considering that the respiratory virus is contagious, this mechanism is designed to be disposable, featured with low cost, easy fabrication, and simple assembly. Since the device is made of single material, its sterilization process can be simplified irrespective of electrical short or erosion. According to the experimental results, the generated force is considerably constant (0.67±0.04 N and 0.57±0.02 N) during a 20 mm stroke. There is a small difference of force during the compression and return of the mechanism. The reason can be the friction between the slider and the column guide. In practice, the mechanism can be made by molding, and the smoothness of the sliding surface can be improved. Also, the increasing trend in the compression can be due to the material hysteresis. Additional design optimizations are processing and experiments on human subjects are preparing.

References

[1] S.-Q. Li, W.-L. Guo, H. Liu, T. Wang, Y.-Y. Zhou, T. Yu, C.-Y. Wang, Y.-M. Yang, N.-S. Zhong, N.-F. Zhang *et al.*, "Clinical application of an intelligent oropharyngeal swab robot: implication for the covid-19 pandemic," *European Respiratory Journal*, vol. 56, no. 2, 2020.

[2] J. Seo, S. Shim, H. Park, J. Baek, J. H. C. Kim *et al.*, "Development of robot-assisted untact swab sampling system for upper respiratory disease," *Applied Sciences*, vol. 10, no. 21, p. 7707, 2020.

[3] S. Wang, K. Wang, R. Tang, J. Qiao, H. Liu, and Z.-G. Hou, "Design of a low-cost miniature robot to assist the covid-19 nasopharyngeal swab sampling," *IEEE Transactions on Medical Robotics and Bionics*, 2020.

[4] Z. Cheng, S. Foong, D. Sun, and U.-X. Tan, "Towards a multi-dof passive balancing mechanism for upper limbs," in *2015 IEEE International Conference on Rehabilitation Robotics (ICORR)*. IEEE, 2015, pp. 508–513.

[5] P. Bilancia and G. Berselli, "Design and testing of a monolithic compliant constant force mechanism," *Smart Materials and Structures*, vol. 29, no. 4, p. 044001, 2020.

[6] Y.-H. Chen and C.-C. Lan, "An adjustable constant-force mechanism for adaptive end-effector operations," *Journal of Mechanical Design*, vol. 134, no. 3, 2012.

[7] G. Ananthasuresh, "Design of a compliant mechanism to modify an actuator characteristic to deliver a constant output force," *Journal of Mechanical Design*, vol. 128, p. 1101, 2006.

[8] C. V. Jutte and S. Kota, "Design of nonlinear springs for prescribed load-displacement functions," *Journal of Mechanical Design*, vol. 130, no. 8, 2008.

[9] Z. Cheng, S. Foong, D. Sun, and U.-X. Tan, "Algorithm for design of compliant mechanisms for torsional applications," in *2014 IEEE/ASME International Conference on Advanced Intelligent Mechatronics*. IEEE, 2014, pp. 628–633.